

SUPPLEMENTARY INFORMATION

Selective In Vivo Metabolic Cell Labeling Mediated Cancer Targeting

Hua Wang^{b,*}, Ruibo Wang^{b,*}, Kaimin Cai^{b,*}, Hua He^a, Yang Liu^b, Jonathan Yen^c, Zhiyu Wang^b, Ming Xu^b, Yiwen Sun^b, Xin Zhou^d, Qian Yin^b, Li Tang^b, Iwona T. Dobrucki^c, Lawrence W. Dobrucki^c, Eric J. Chaney^f, Stephen A. Boppart^{c,f,g,h}, Timothy M. Fan^{i,1}, Stéphane Lezmi^{j,1}, Xuesi Chen^{p,1}, Lichen Yin^{a,1}, Jianjun Cheng^{a,b,c,k,l,m,n,o,1}

^aJiangsu Key Laboratory for Carbon-Based Functional Materials & Devices, Institute of Functional Nano & Soft Materials (FUNSOM), Soochow University, Suzhou 215123, Jiangsu, China.

^bDepartment of Materials Science and Engineering, ^cDepartment of Bioengineering,

^eMolecular Imaging Laboratory, Beckman Institute for Advanced Science and Technology,

^fBiophotonics Imaging Laboratory, Beckman Institute for Advanced Science and Technology,

^gDepartment of Electrical and Computer Engineering, ^hDepartment of Internal Medicine,

ⁱDepartment of Veterinary Clinical Medicine, ^jDepartment of Pathobiology at College of

Veterinary Medicine, ^kDepartment of Chemistry, ^lBeckman Institute for Advanced Science and

Technology, ^mMicro and Nanotechnology Laboratory, ⁿInstitute of Genomic Biology, ^oMaterials Research Laboratory, University of Illinois at Urbana–Champaign, Urbana, IL, 61801, USA.

^dDepartment of Chemistry, University of Science and Technology of China, Hefei, Anhui 230026, China.

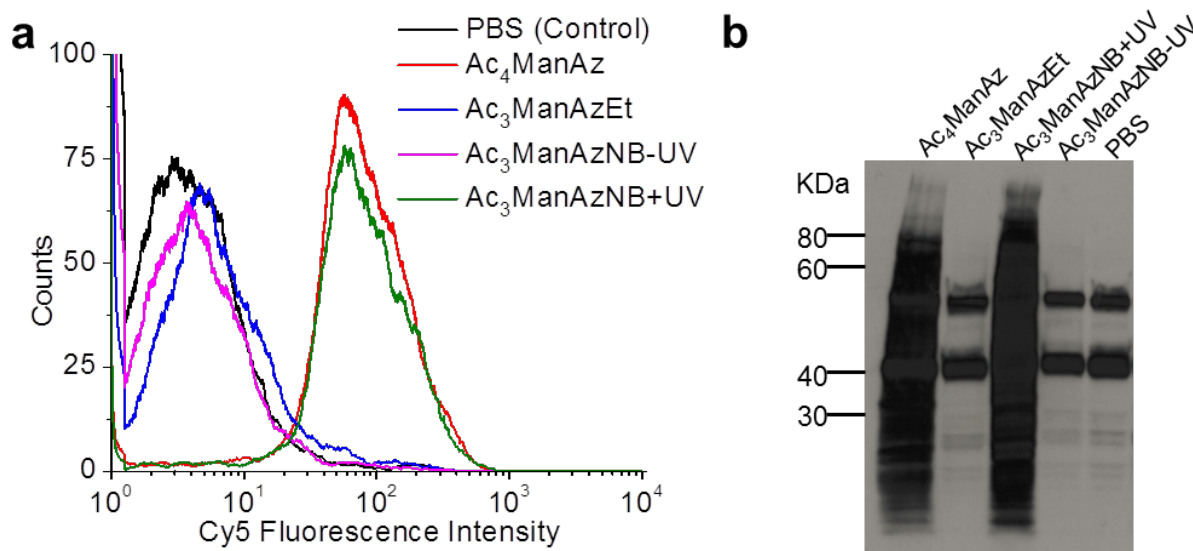
^pKey Laboratory of Polymer Ecomaterials, Changchun Institute of Applied Chemistry, Changchun 130022, People's Republic of China

*These authors contributed equally to this work.

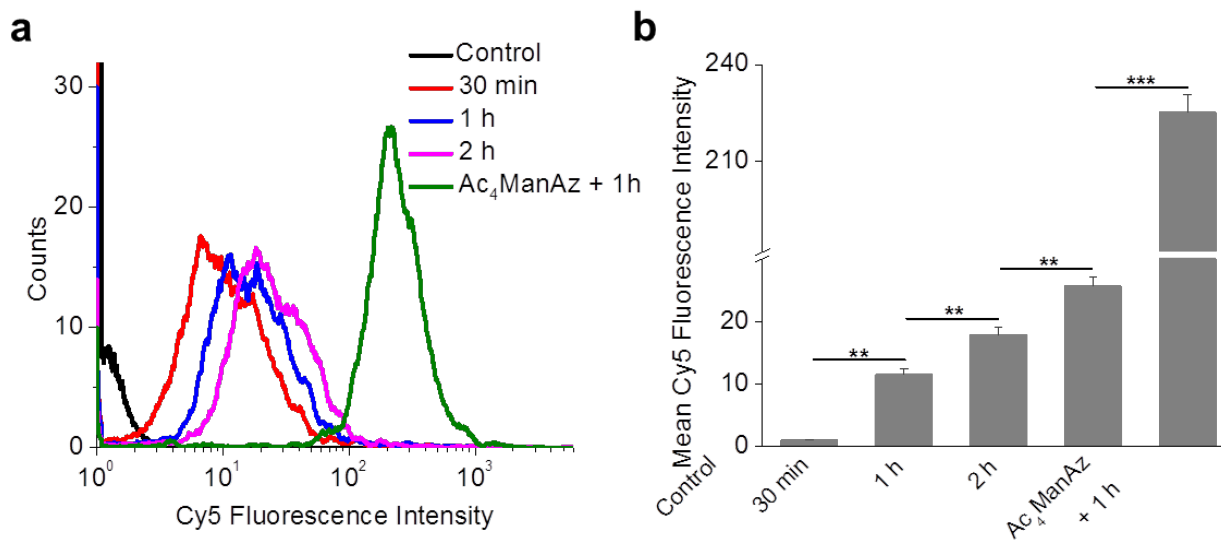
¹To whom correspondence may be addressed. Email: jianjunc@illinois.edu; leyin@suda.edu.cn; xschen@ciac.ac.cn; slezmi@illinois.edu; t-fan@illinois.edu.

SUPPLEMENTARY RESULTS

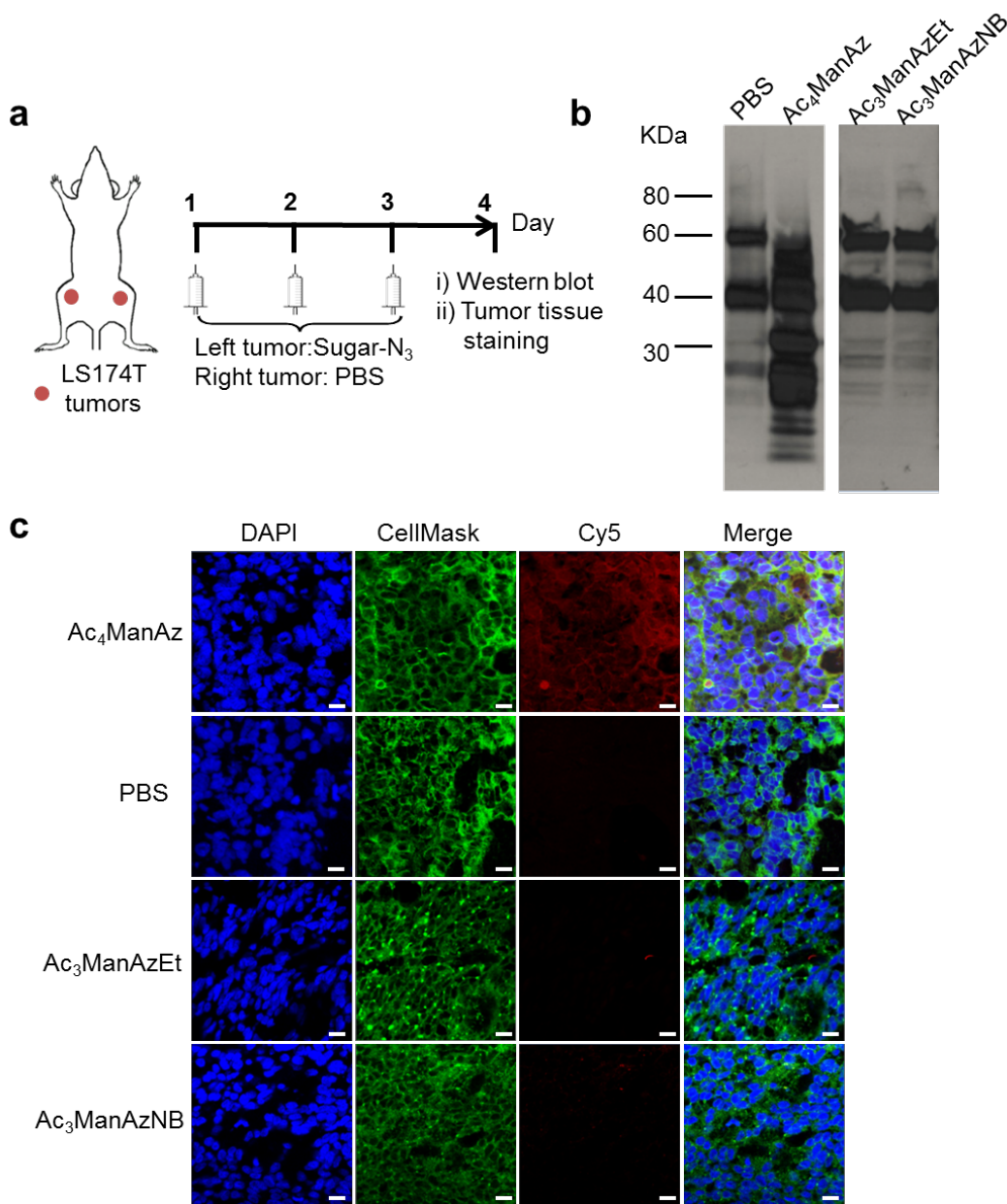
SUPPLEMENTARY FIGURES



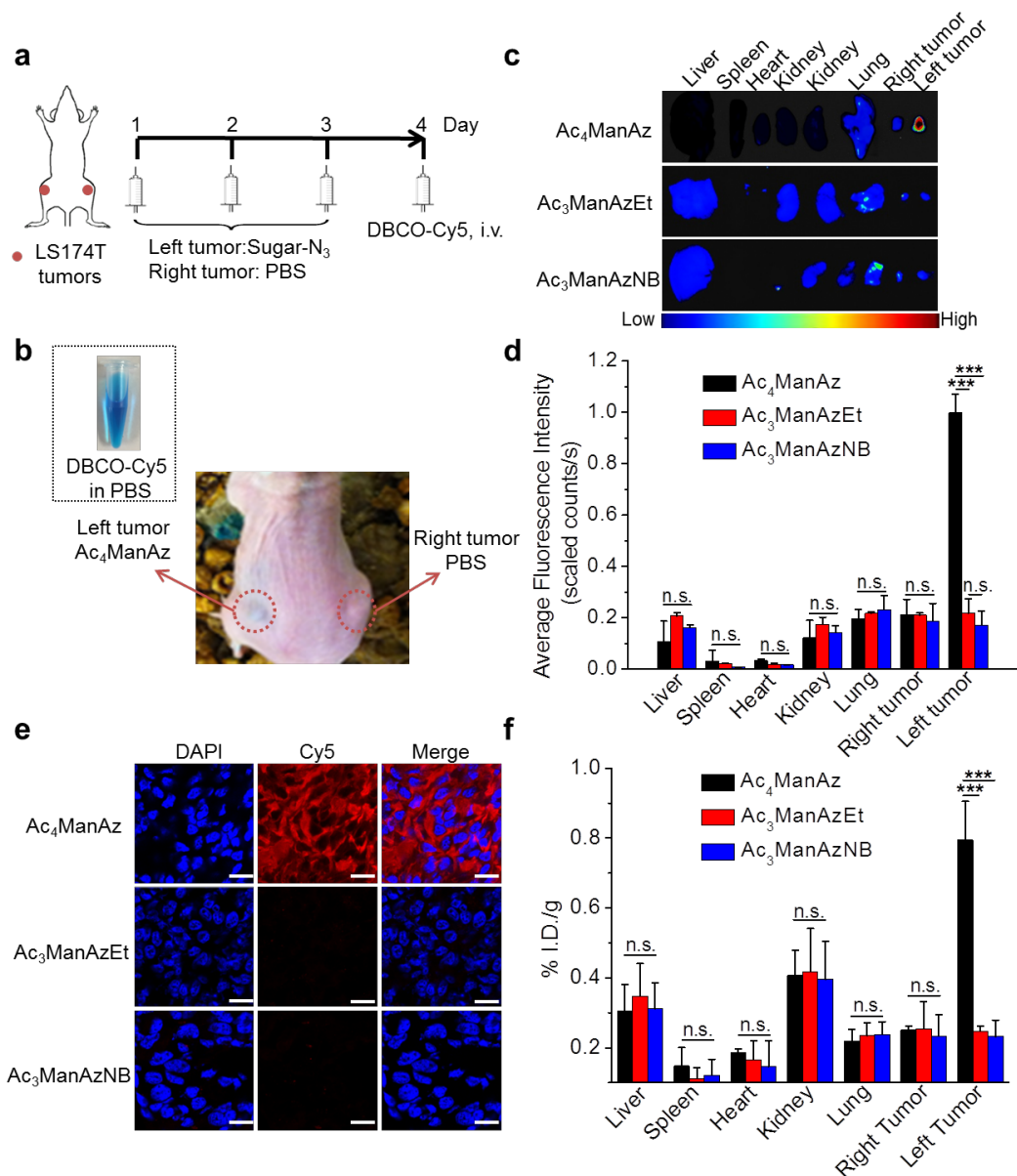
Supplementary Figure 1. Replacing the C1-OAc of Ac₄ManAz with a cleavable ether bond enabled controlled metabolic cell labeling in vitro. (a) Flow cytometry analysis of LS174T cells after treated with PBS, Ac₄ManAz, Ac₃ManAzEt, Ac₃ManAzNB-UV, and Ac₃ManAzNB+UV, respectively, for 72 h and labeled with DBCO-Cy5 for 1 h. UV irradiation with an intensity of 10 mW/cm² was applied for 10 min at the start of incubation. (b) Western blotting analysis of LS174T cells after treatment with Ac₄ManAz, Ac₃ManAzEt, Ac₃ManAzNB+UV, Ac₃ManAzNB-UV, and PBS, respectively, for 72 h. Azido-modified proteins were biotinylated by incubating with phosphine-PEG₄-biotin and then detected by streptavidin-horseradish peroxidase conjugate. Ac₃ManAzEt, Ac₃ManAzNB and PBS groups showed only two endogenous biotinylated protein bands.



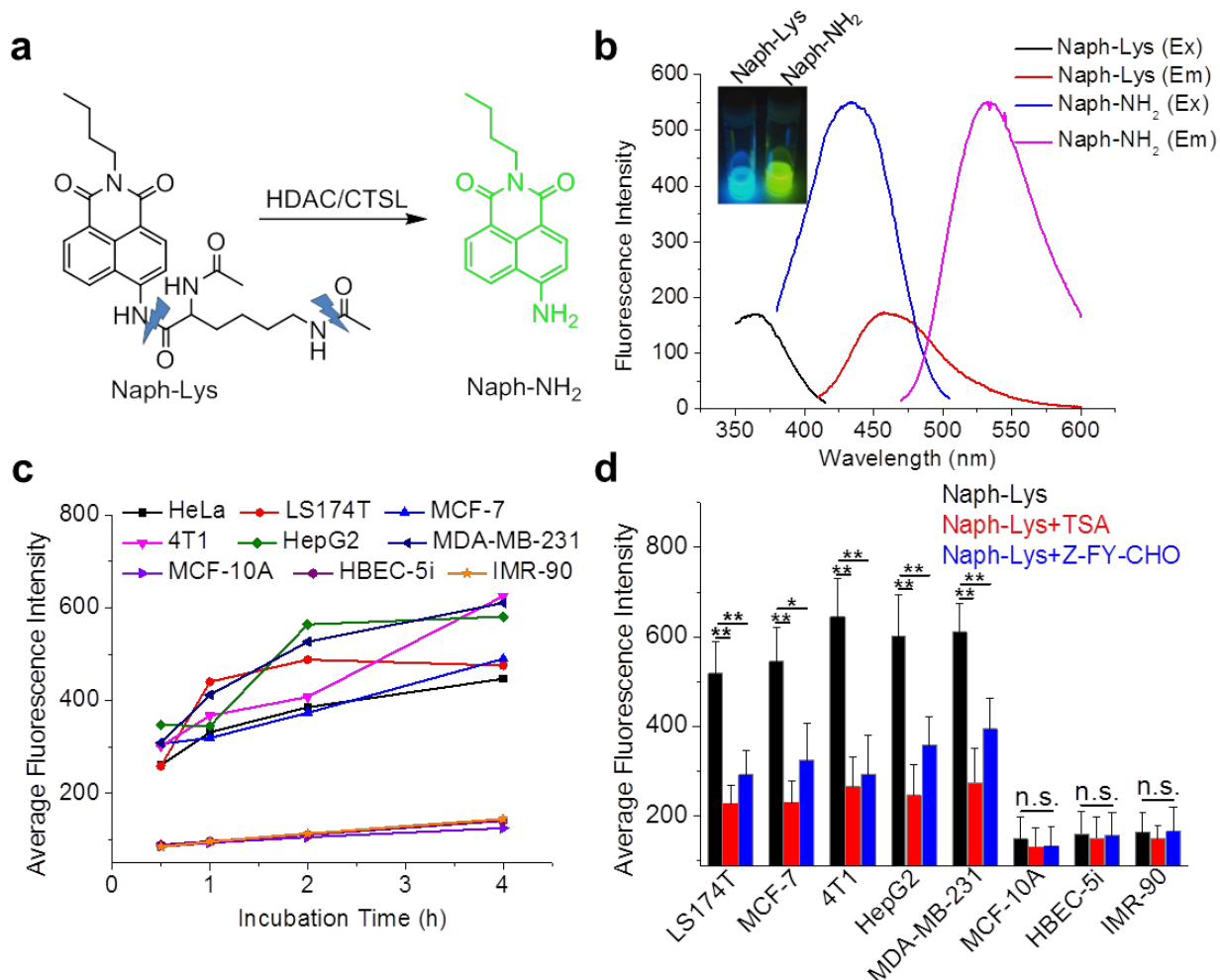
Supplementary Figure 2. Comparison of active and passive uptake of DBCO-Cy5. (a) Flow cytometry analyses of LS174T cells after incubation with DBCO-Cy5 for 30 min, 1 h, and 2 h, respectively. Cells without DBCO-Cy5 treatment were used as negative controls. Cells pretreated with Ac₄ManAz (50 μ M) for three days and further treated with DBCO-Cy5 for 1 h were used for comparison. (b) Mean fluorescence intensity of LS174T cells for different groups in (a). Data were presented as mean \pm SEM (n=6) and analyzed by one-way ANOVA (Fisher; $0.01 < *P \leq 0.05$; $**P \leq 0.01$; $***P \leq 0.001$).



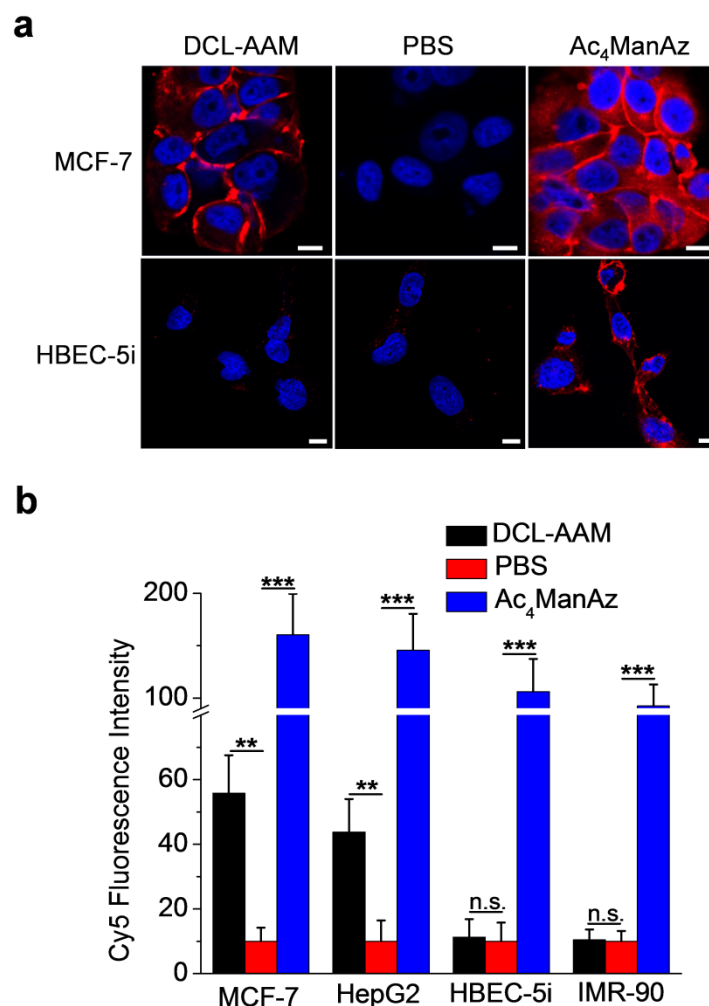
Supplementary Figure 3. Ac₃ManAzEt and Ac₃ManAzNB showed blocked metabolic labeling activity in vivo. (a) Time course of in vivo labeling study in athymic nude mice bearing subcutaneous LS174T tumors. When the tumors reached ~50 mm³, Ac₄ManAz or Ac₃ManAzEt or Ac₃ManAzNB (25 mM, 20 μL) was injected to the left tumors once daily for three days. The right tumors were injected with PBS as controls. (b) Western blotting analysis of tumor tissues treated with PBS, Ac₄ManAz, Ac₃ManAzEt, and Ac₃ManAzNB, respectively. Azido-modified proteins were first biotinylated by incubating with phosphine-PEG₄-biotin, and then detected by streptavidin-horseradish peroxidase conjugate. (c) CLSM images of tumor tissue sections from different groups. Tumor tissues were blocked with BSA for 2 h and then labeled with DBCO-Cy5 (red) for 30 min. Cell nuclei and membrane were stained with DAPI (blue) and CellMask orange plasma membrane stain (green), respectively. Scale bar: 10 μm.



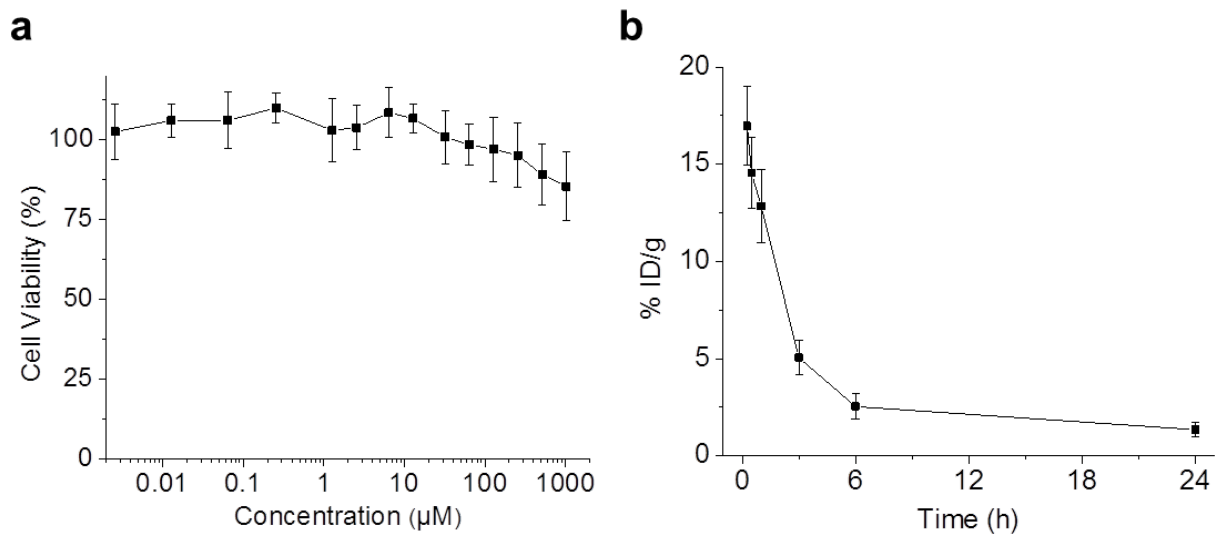
Supplementary Figure 4. Tumor accumulation of DBCO-Cy5 was significantly improved in azido-modified tumors. (a) Time course of in vivo labeling study in athymic nude mice bearing subcutaneous LS174T tumors. Sugar-N₃ (25 mM, 20 μ L) was injected to the left tumors once daily for three days (Day 1-3), and the right tumors were injected with PBS as controls. DBCO-Cy5 (5 mg/kg) was i.v. injected on Day 4, and mice were sacrificed for analysis at 48 h p.i. of DBCO-Cy5. (b) Picture of mouse at 48 h p.i. of DBCO-Cy5. The left tumor injected with Ac₄ManAz showed the intrinsic blue color of DBCO-Cy5, and the right tumor injected with PBS showed no blue color. A picture of DBCO-Cy5 solution was shown. (c) Fluorescence imaging of harvested tissues from different group mice. (d) Fluorescence intensity of tissues (n=3) from (c). (e) CLSM images of tumor tissue sections from different groups. The cell nuclei were stained with DAPI (blue). Scale bar: 20 μ m. (f) Retained Cy5 in tissues from different groups (n=3). All of the numerical data were presented as mean \pm SEM and analyzed by one-way ANOVA (Fisher; 0.01 < *P \leq 0.05; **P \leq 0.01; ***P \leq 0.001).



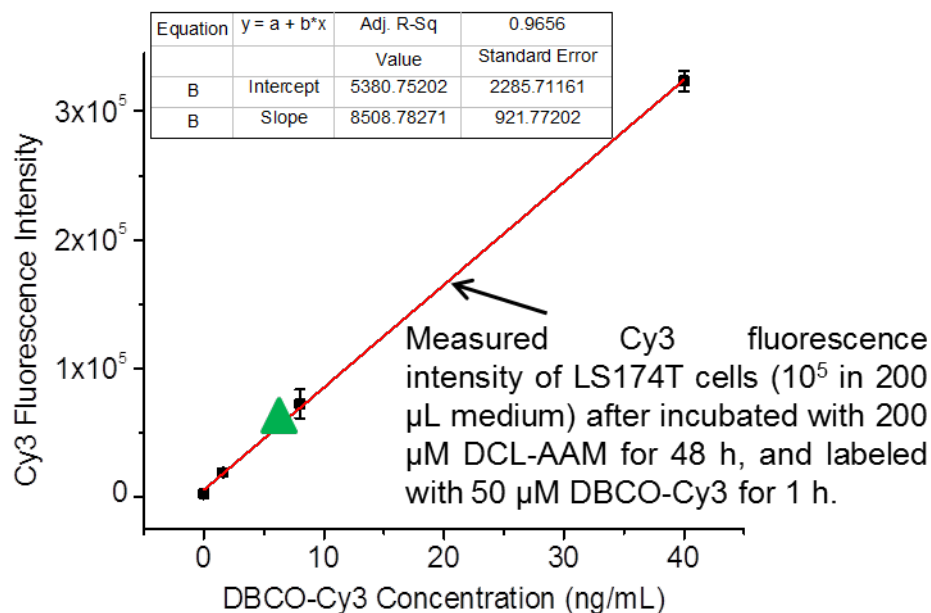
Supplementary Figure 5. HDAC and CTSL are overexpressed in various cancer cell lines. (a) Structure of the HDAC/CTSL fluorescence turn-on reporter (Naph-Lys) and its degradation product (Naph-NH₂) in the presence of HDAC/CTSL. (b) Excitation and emission spectra of Naph-Lys (5 μg/mL in methanol) and Naph-NH₂ (200 ng/mL in methanol). (c) Detection of HDAC/CTSL activity in different cell lines (HeLa, black; LS174T, red; MCF-7, blue; 4T1, magenta; HepG2, olive; MDA-MB-231, navy; MCF-10A, violet; HBEC-5i, purple; IMR-90, orange). (d) Average fluorescence intensity of different cell lines treated with Naph-Lys (50 μM), Naph-Lys (50 μM) + TSA (1 μM), and Naph-Lys (50 μM) + Z-FY-CHO (50 μM), respectively, for 4 h. Data were presented as mean ± SEM (n=6) and analyzed by one-way ANOVA (Fisher; 0.01 < *P ≤ 0.05; **P ≤ 0.01; ***P ≤ 0.001).



Supplementary Figure 6. DCL-AAM mediated cancer-selective labeling in vitro. (a) CLSM images of MCF-7 breast cancer cells (upper row) and HBEC-5i cerebral microvascular endothelium cells (lower row) after incubated with DCL-AAM (50 μ M) or PBS or Ac₄ManAz (50 μ M) for 72 h and labeled with DBCO-Cy5 (50 μ M) for 1 h. The cell nuclei were stained with DAPI (blue). Scale bar: 10 μ m. (b) Average Cy5 fluorescence intensity of different cell lines (MCF-7, HepG2, HBEC-5i, and IMR-90 cells) following the same treatment as described in (a). Data were presented as mean \pm SEM (n=6) and analyzed by one-way ANOVA (Fisher; 0.01 < * P \leq 0.05; ** P \leq 0.01; *** P \leq 0.001).

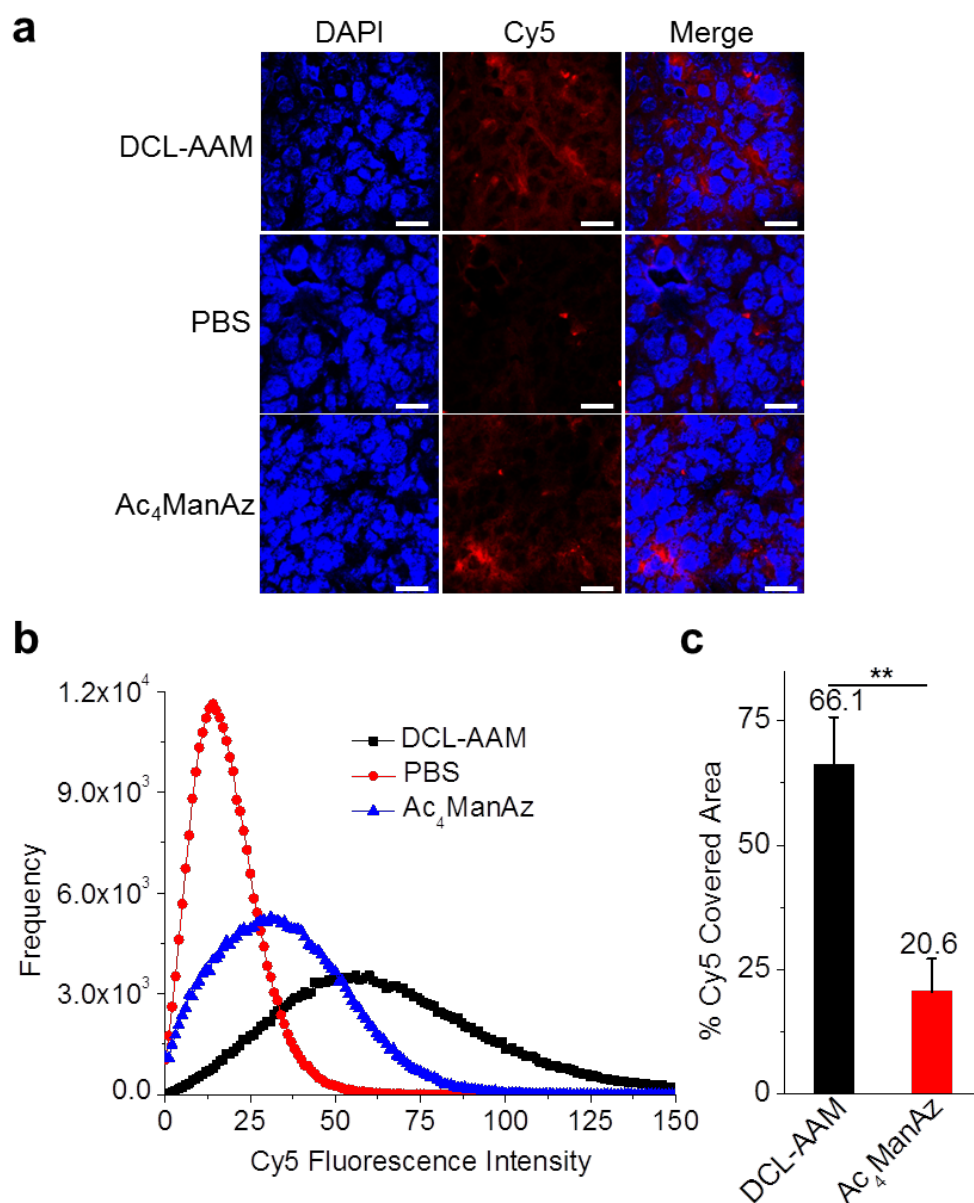


Supplementary Figure 7. DCL-AAM showed minimum cytotoxicity and short circulation half-life. (a) Cell Viability of LS174T cells after treated with different concentrations of DCL-AAM for 72 h, as determined by MTT assay. (c) Pharmacokinetic profile of ^{64}Cu -labeled E-S in athymic nude mice.

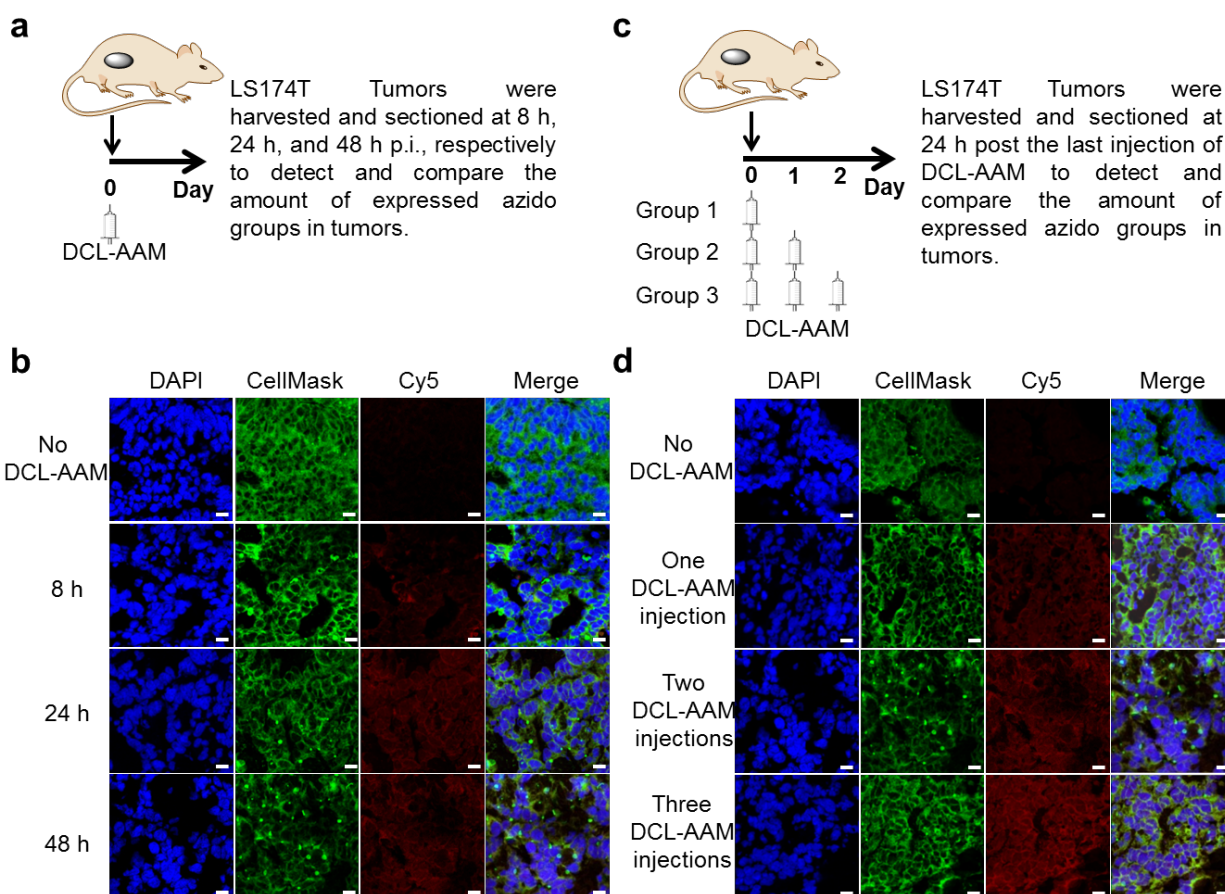


Mass of DBCO-Cy3 per cell: $(7.5 \text{ ng/mL} * 200 \mu\text{L})/100000 \text{ cells} = 1.5 * 10^{-5} \text{ ng/cell}$
 Moles of azides per cell: $(1.5 * 10^{-5} \text{ ng/cell})/(983.18 \text{ g/mol}) = 1.5 * 10^{-17} \text{ mol}$
 Number of azides per cell: $1.5 * 10^{-17} \text{ moles} * (6.02 * 10^{23} \text{ mol}^{-1}) = 9.0 * 10^6$

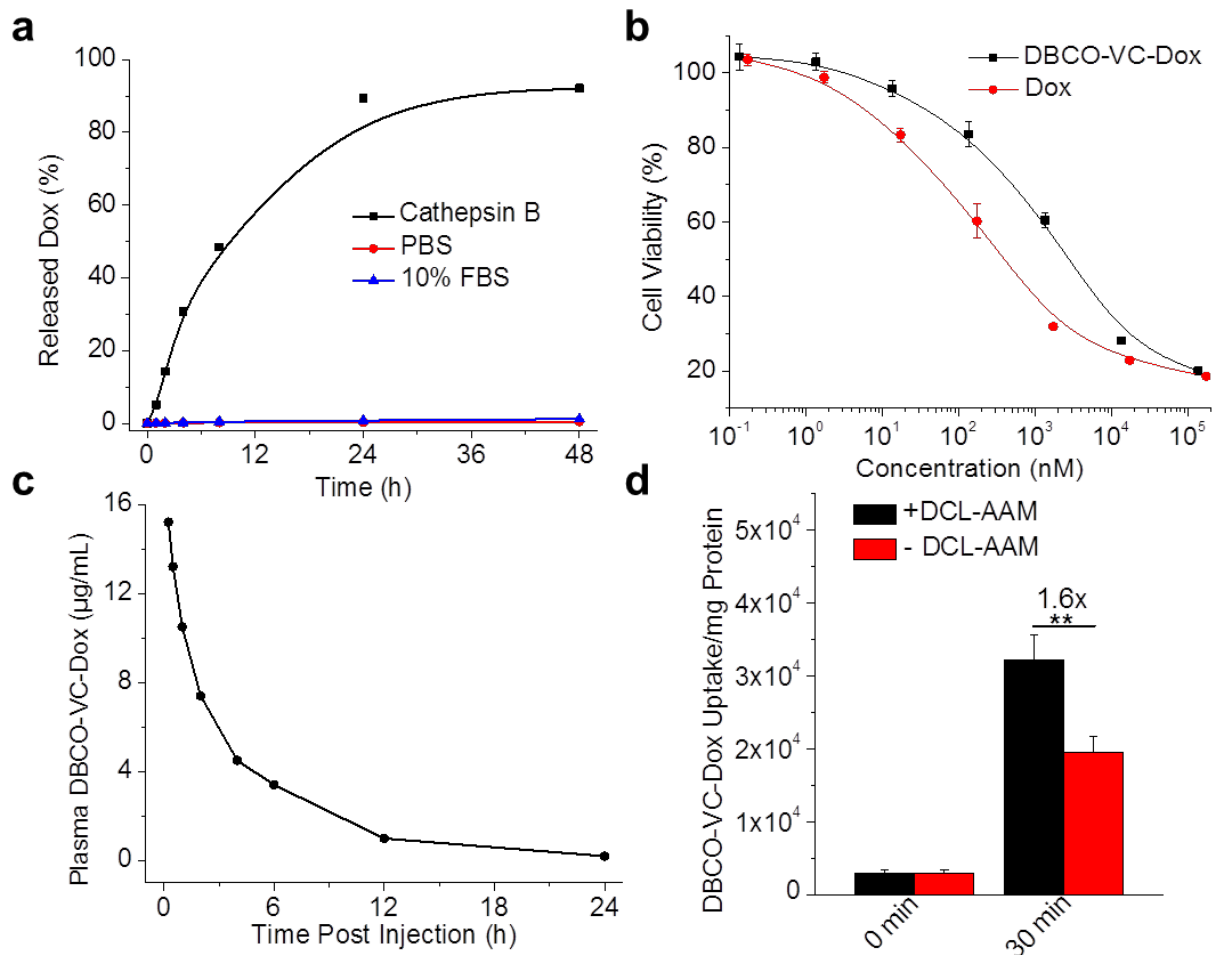
Supplementary Figure 8. Estimation of number density of azido groups on the surface of LS174T cells after incubated with $200 \mu\text{M}$ DCL-AAM for 48 h and labeled with $50 \mu\text{M}$ DBCO-Cy3 for 1 h.



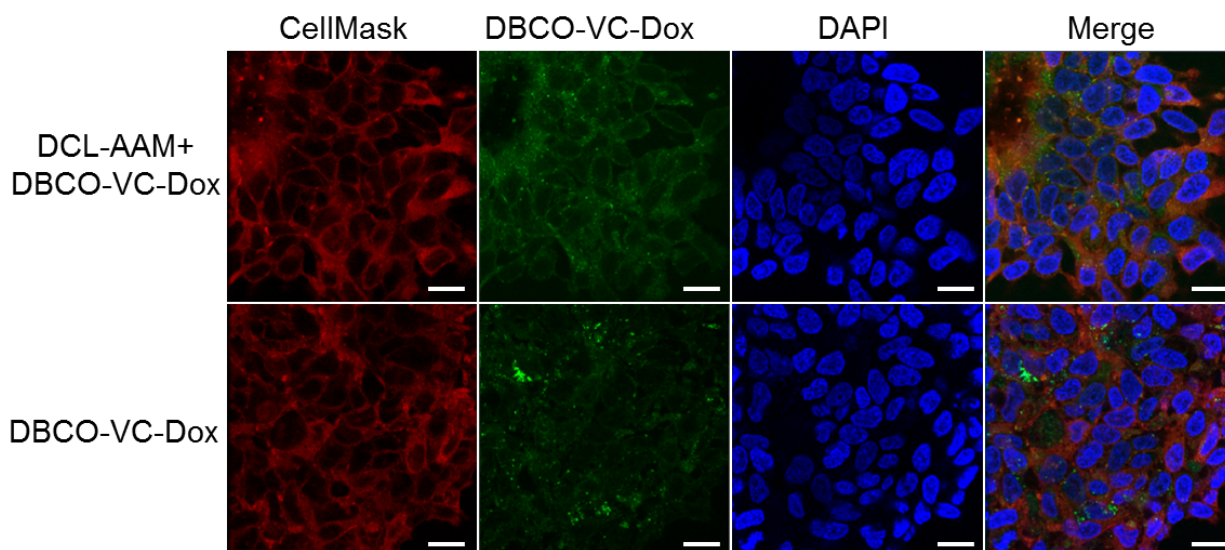
Supplementary Figure 9. DCL-AAM showed superior in vivo cancer-selective labeling capability in comparison with Ac₄ManAz. DCL-AAM (60 mg/kg), Ac₄ManAz (40 mg/kg) or PBS was i.v. injected into athymic nude mice bearing subcutaneous LS174T tumors once daily for three days. DBCO-Cy5 (10 mg/kg) was i.v. injected at 24 h post the last injection of azido-sugars. Mice were sacrificed at 48 h p.i. of DBCO-Cy5. (a) CLSM images of tumor sections from mice treated with DCL-AAM, Ac₄ManAz, and PBS, respectively. The cell nuclei were stained with DAPI (blue). Scale bar: 20 μ m. (b) Cy5 fluorescence intensity profiles of tumor sections extracted from (a) and averaged over 20 images. (c) Percentage of Cy5-covered area of tumor tissue sections which was calculated from (b) and defined as: the sum of frequency (Cy5 fluorescence intensity \geq 50 a.u.) divided by the total frequency.



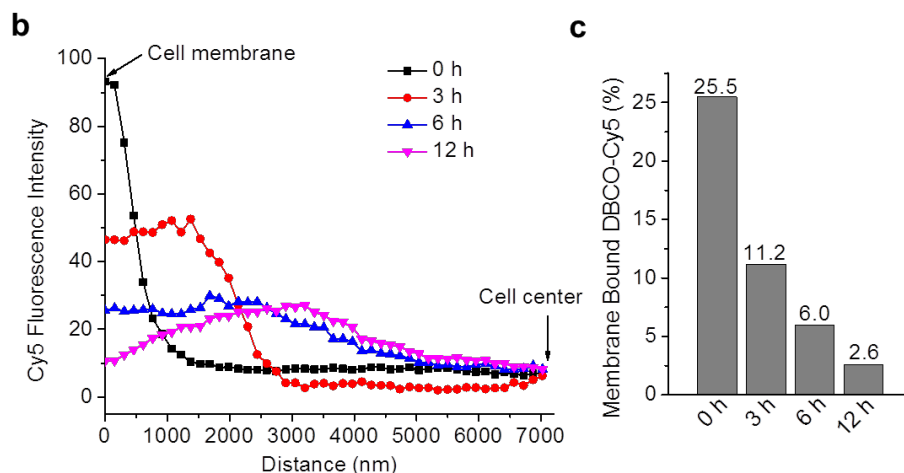
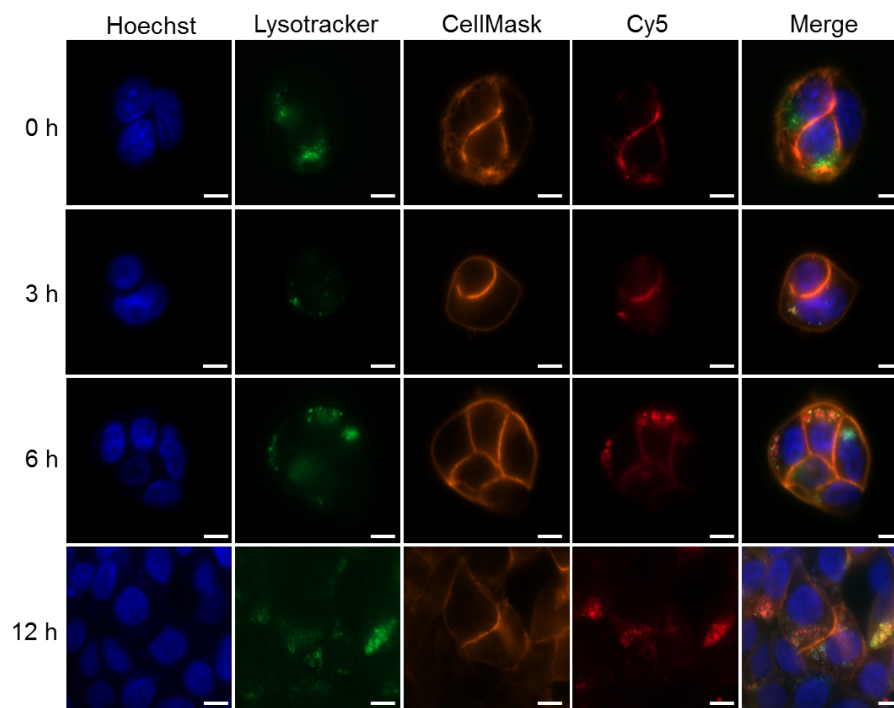
Supplementary Figure 10. DCL-AAM mediated tumor labeling in vivo was time- and dose frequency-dependent. (a-b): In vivo tumor labeling kinetics of DCL-AAM. (a) Time course of in vivo labeling kinetics study. Athymic nude mice bearing subcutaneous LS174T tumors were i.v. injected with DCL-AAM (60 mg/kg). Tumors were harvested and sectioned at 8, 24, and 48 h p.i. of DCL-AAM, respectively, for determining the time-course expression profiles of azido groups. (b) CLSM images of tumor tissue sections harvested at 8, 24, and 48 h p.i. of DCL-AAM (60 mg/kg), respectively. Tumor tissue sections were blocked with 5% BSA for 2 h and then labeled with DBCO-Cy5 (red) for 30 min. Cell nuclei and membrane were stained with DAPI (blue) and CellMask orange plasma membrane stain (green), respectively. Scale bar: 10 μ m. (c-d): Dose frequency-dependent DCL-AAM mediated tumor labeling in vivo. (c) Time course of in vivo labeling study. Athymic nude mice bearing subcutaneous LS174T tumors were i.v. administered with DCL-AAM (60 mg/kg) for once, twice, and three times, respectively. Tumors were harvested and sectioned at 24 h post the last injection of DCL-AAM. (d) CLSM images of tumor tissue sections harvested from athymic nude mice with 0, 1, 2, and 3 injections of DCL-AAM, respectively, following the same treatment as described in (b). Scale bar: 10 μ m.



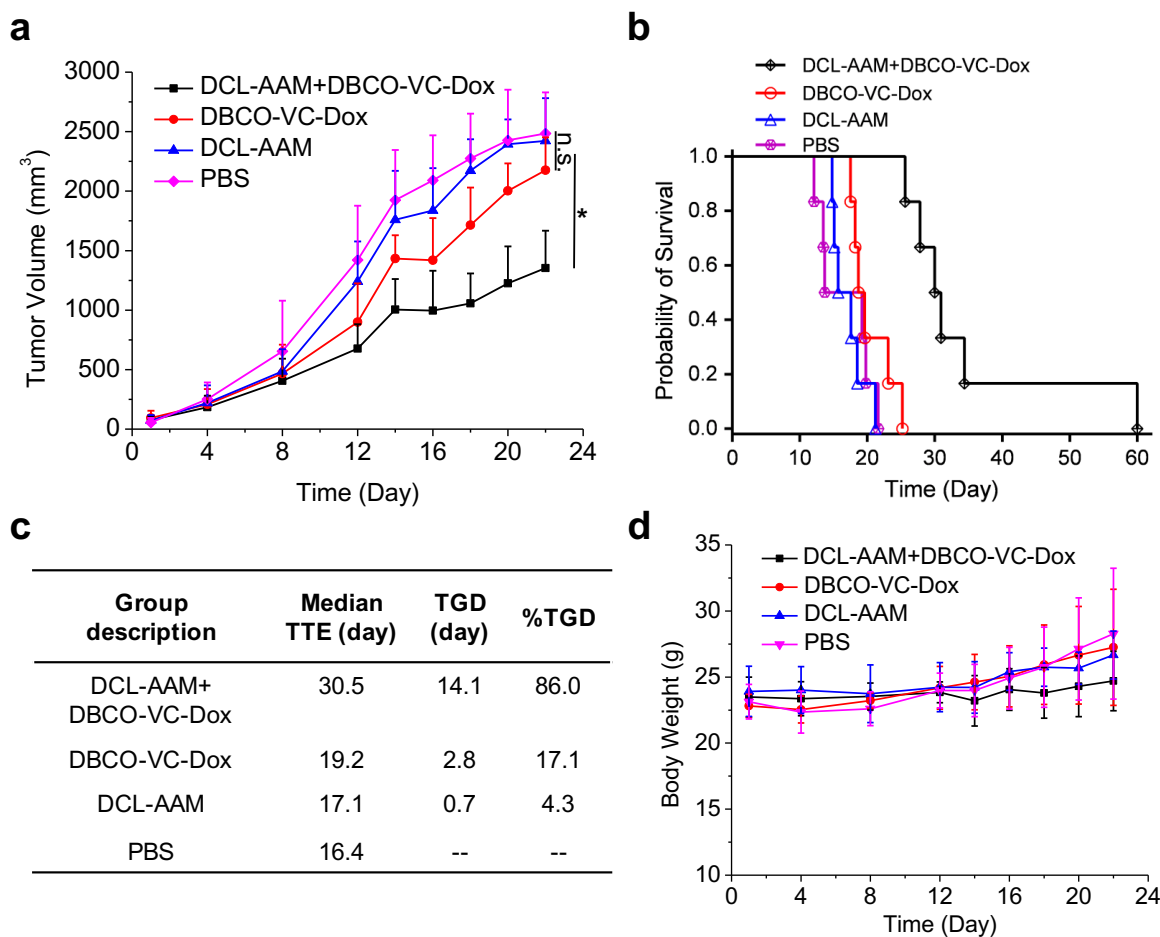
Supplementary Figure 11. Characterizations of DBCO-VC-Dox. (a) Release profile of DBCO-VC-Dox in the presence of activated cathepsin B, PBS, and 10% FBS, respectively. (b) Viability of LS174T cells after treated with DBCO-VC-Dox or Dox at various concentrations for 72 h. The data were presented as mean \pm SEM, $n = 6$. (c) Pharmacokinetic profiles of DBCO-VC-Dox in athymic nude mice. (d) DBCO-VC-Dox uptake by LS174T cells with or without DCL-AAM pretreatment (72 h) over 30-min incubation. Cells without DBCO-VC-Dox treatment (0 min) were used as negative controls. Data were presented as mean \pm SEM ($n=6$) and analyzed by one-way ANOVA (Fisher; $0.01 < *P \leq 0.05$; $**P \leq 0.01$; $***P \leq 0.001$).



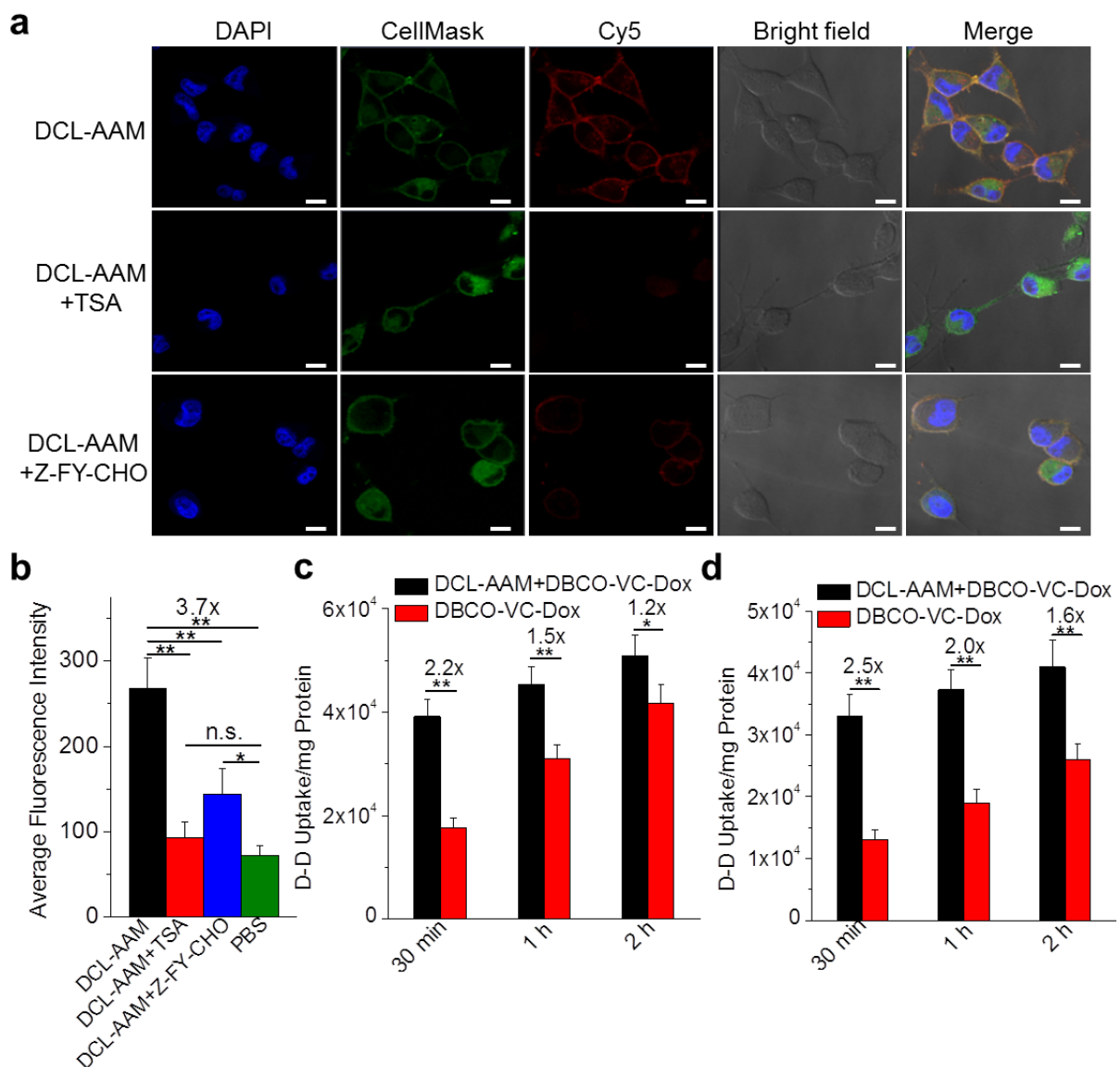
Supplementary Figure 12. DBCO-VC-Dox was partially covalently attached to DCL-AAM treated LS174T cells. LS174T cells were pretreated with DCL-AAM (50 μ M) or PBS for three days, labeled with DBCO-VC-Dox (20 μ M) for 1 h, and imaged under a confocal microscope. Cell membrane and nuclei were stained with CellMask deep red plasma membrane stain (red) and DAPI (blue), respectively. Scale bar: 10 μ m.



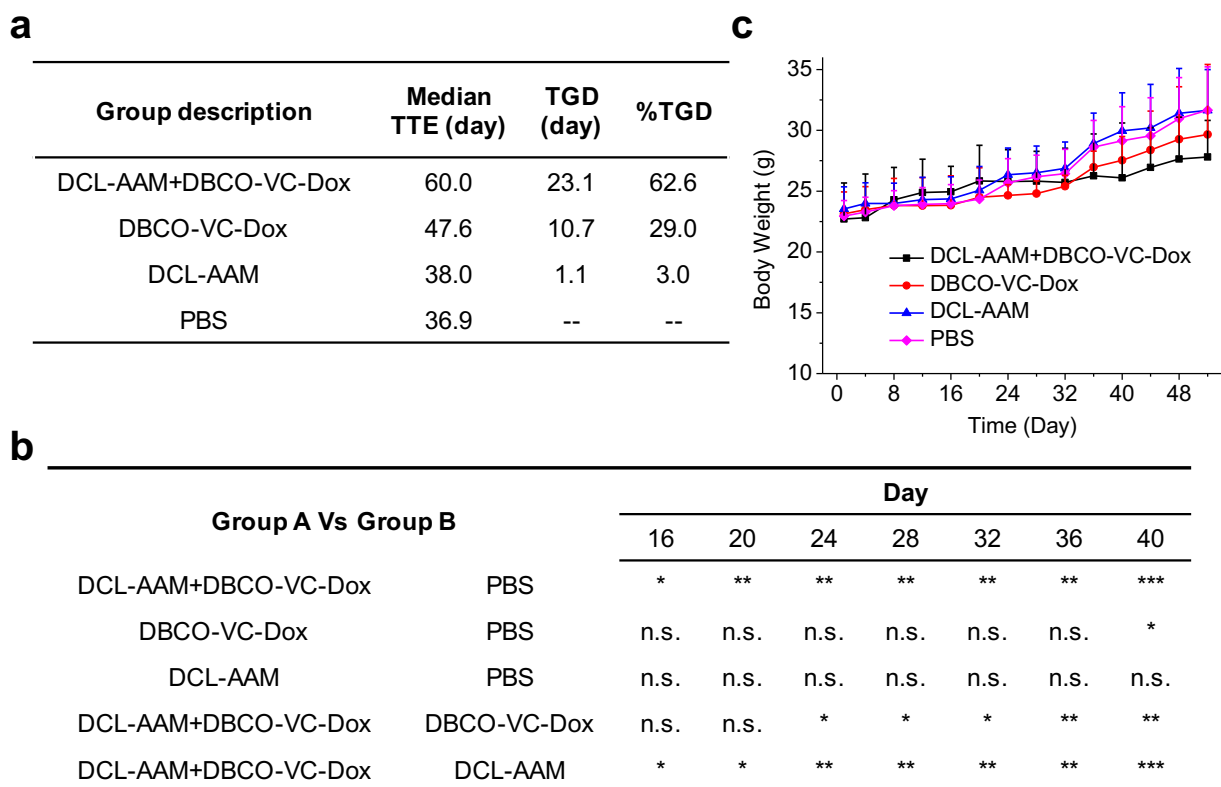
Supplementary Figure 13. Covalently attached DBCO-Cy5 entered endosomes/lysosomes in DCL-AAM treated LS174T cells. LS174T cells were pretreated with DCL-AAM (50 μ M) for three days and labeled with DBCO-Cy5 (50 μ M) for 1 h. After washing with PBS, cells were further incubated in fresh medium for different time (0, 3, 6, and 12 h) and imaged under a fluorescence microscope. (a) CLSM images of LS174T cells that were further incubated for 0, 3, 6, and 12 h, respectively. Endosomes/lysosomes were stained with Lysotracker green (green). Cell membrane and nuclei were stained with CellMask orange plasma membrane stain (orange) and Hoechst 33342 (blue), respectively. Scale bar: 10 μ m. (b) Cy5 fluorescence intensity profile over the longitudinal direction of cells from (a). For each cell, the Cy5 fluorescence intensity profile over the longitudinal direction was extracted from CLSM image using ZEN software, with the longitudinal diameter of cell normalized to 14.5 μ m. The profiles were then averaged over 30 cells for each group. (c) Percentage of membrane-bound DBCO-Cy5 for different further-incubation time, as calculated from (b) and defined as the sum of Cy5 fluorescence counts of 100-7000 nm interval divided by the total fluorescence counts of 0-7000 nm.



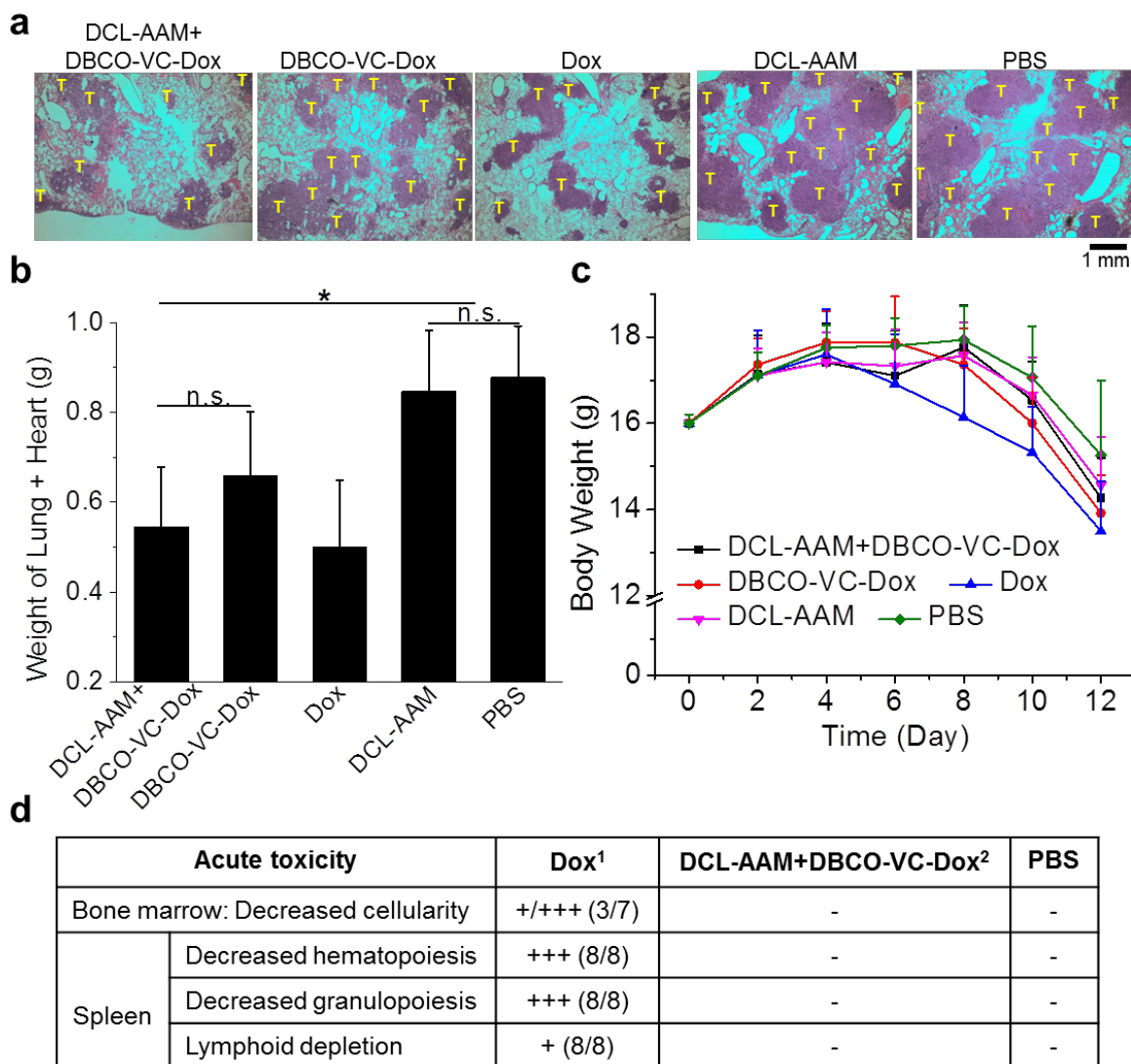
Supplementary Figure 14. DCL-AAM mediated tumor labeling significantly improved long-term antitumor efficacy of DBCO-VC-Dox against subcutaneous LS174T tumors in athymic nude mice. LS174T tumors were established in 6 week-old female athymic nude mice by subcutaneous injection of LS174T cells into both flanks. When the tumors reached ~50 mm³, mice were randomly divided into 4 groups (group 1: DCL-AAM+DBCO-VC-Dox; group 2: DBCO-VC-Dox; group 3: DCL-AAM; group 4: PBS; n = 5-6). DCL-AAM (60 mg/kg) was i.v. injected on Day 0, 1, and 2. DBCO-VC-Dox (12 mg/kg in Dox equivalent) was i.v. injected on Day 3, 7, and 11. Tumor volume and body weight were measured every other day. (a) Average LS174T tumor volume of mice from different groups over the course of the efficacy study. Data were presented as mean \pm SEM (n=10) and analyzed by one-way ANOVA (Fisher; $0.01 < *P \leq 0.05$; $**P \leq 0.01$; $***P \leq 0.001$). (b) Kaplan-Meier plots for all groups. Loss of mice was because of treatment-related death or euthanasia after the predetermined end point was reached. (c) Survival analysis of mice from different groups. TTE: time to end point. TGD: tumor growth delay; TGD = TTE (treated group) – TTE (PBS group). %TGD = $100\% \times \text{TGD}/\text{TTE}$ (PBS group). (d) Body weight of mice from different groups over the course of the efficacy study.



Supplementary Figure 15. DCL-AAM could efficiently label MDA-MB-231 and 4T1 cells and resulted in enhanced uptake of DBCO-VC-Dox in vitro. (a) CLSM images of MDA-MB-231 cells after incubated with DCL-AAM (50 μ M), DCL-AAM (50 μ M) + TSA (1 μ M), and DCL-AAM (50 μ M) + Z-FY-CHO (50 μ M), respectively, for 72 h and labeled with DBCO-Cy5 (50 μ M) for 1 h. The cell nuclei and membrane were stained with DAPI (blue) and CellMask orange plasma membrane stain (green), respectively. Scale bar: 10 μ m. (b) Average Cy5 fluorescence intensity of MDA-MB-231 cells following the same treatment in (a). DBCO-VC-Dox uptake by MDA-MB-231 cells (c) and 4T1 cells (d) with or without DCL-AAM pretreatment (72 h) over different incubation time (30 min, 1 h, and 2 h). All the numerical data were presented as mean \pm SEM (n=6) and analyzed by one-way ANOVA (Fisher; 0.01 < *P \leq 0.05; **P \leq 0.01; ***P \leq 0.001).



Supplementary Figure 16. DCL-AAM mediated tumor labeling significantly improved long-term antitumor efficacy of DBCO-VC-Dox against subcutaneous MDA-MB-231 tumors in athymic nude mice. MDA-MB-231 tumors were established in 6 week-old female athymic nude mice by subcutaneous injection of MDA-MB-231 cells into both flanks. When the tumors reached $\sim 50 \text{ mm}^3$, mice were randomly divided into 4 groups (group 1: DCL-AAM+DBCO-VC-Dox; group 2: DBCO-VC-Dox; group 3: DCL-AAM; group 4: PBS; $n = 5$). DCL-AAM was i.v. injected on Day 0, 1, and 2. Subsequently DBCO-VC-Dox was i.v. injected on Day 3, 7, and 11. (a) Survival analysis of mice from different groups. TTE: time to end point. TGD: tumor growth delay; $\text{TGD} = \text{TTE} (\text{treated group}) - \text{TTE} (\text{PBS group})$. $\% \text{TGD} = 100\% \times \text{TGD} / \text{TTE} (\text{PBS group})$. (b) Statistical analyses of the tumor volume by one-way ANOVA and Fisher's LSD test ($0.01 < *P \leq 0.05$; $**P \leq 0.01$; $***P \leq 0.001$). (c) Body weight of mice from different groups over the course of the efficacy study. Curves were truncated when three or more mice were dead or sacrificed.



Supplementary Figure 17. DCL-AAM mediated cancer labeling significantly improved anticancer efficacy of DBCO-VC-Dox against 4T1 lung metastases in BALB/c mice. Luciferase-engineered 4T1 cells were i.v. injected into BALB/c mice on Day 0, and mice were randomly divided into 5 groups (group 1: DCL-AAM+DBCO-VC-Dox; group 2: DBCO-VC-Dox; group 3: Dox; group 4: DCL-AAM; group 5: PBS; n = 7-8). DCL-AAM (60 mg/kg) was i.v. injected once daily for three days (Day 1, 2, and 3). DBCO-VC-Dox (12 mg/kg in Dox equivalent) or Dox (7.5 mg/kg, maximum tolerated dose) was i.v. injected on Day 4, 8, and 12. (a) Representative images of H&E stained lung tissues of mice from different groups. T indicates tumor. Scale bar: 1 mm. (b) Weight of lung plus heart of mice from different groups (n=7-8). Statistical analyses were conducted by one-way ANOVA (Fisher; $0.01 < *P \leq 0.05$; $**P \leq 0.01$; $***P \leq 0.001$). (c) Body weight of BALB/c mice from different groups over the course of efficacy study. (d) Toxicity evaluation of Dox and DCL-AAM+DBCO-VC-Dox in BALB/c mice. ¹22.5 mg/kg Dox; ²36.0 mg/kg Dox; + (mild); +++ (marked); - (negative).